Applied Acoustics 127 (2017) 240–249

Contents lists available at ScienceDirect

Applied Acoustics

journal homepage: www.elsevier.com/locate/apacoust

Experimental investigation of the far-field noise due to jet-surface interaction combined with a chevron nozzle

Leopoldo P. Bastos [a], Cesar J. Deschamps [b], Andrey R. da Silva [c,*]

[a] Research Group in Acoustics, Thermal Fluid Dynamic and Mechanical Systems, Federal University of Pará, Brazil
[b] Research Laboratories for Emerging Technologies in Cooling and Thermophysics – POLO, Federal University of Santa Catarina, Florianópolis, SC 88040-900, Brazil
[c] Vibrations & Acoustics Laboratory – LVA, Federal University of Santa Catarina, Florianópolis, SC 88040-900, Brazil

ARTICLE INFO

Article history:
Received 4 November 2016
Received in revised form 18 May 2017
Accepted 12 June 2017
Available online 26 June 2017

Keywords:
Jet-surface interaction
Chevron nozzle
Installed jet
Shielding effect

ABSTRACT

High-speed jets exhausting from engines, especially during takeoff, remain one of the main sources of external aircraft noise. Regulations on aircraft noise levels in regions close to airports are very strict and are forcing the aerospace industry to develop quieter aircrafts. Mixing enhancement devices at the exit of nozzles, such as chevrons, have assisted in the reduction of noise levels for some time. However, installation effects are becoming more intense due to highly integrated aircraft-engine configurations, which are currently employed by the aviation industry as an attempt to increase the aerodynamic efficiency and to reduce noise. Consequently, these installation effects may interfere with the noise reducing performance of such devices. This paper reports experimental investigations involving the combined effect of a flat plate integrated with nozzles, both with and without chevrons, exhausting cold subsonic jets. Assessment of the far-field noise was conducted for different Mach numbers and several configurations formed by relative positions between the nozzle and the plate. In general, it was observed that the acoustic benefit of chevrons, as found in isolated jets, remains effective in most of installed configurations. Nevertheless, for highly integrated configurations the low-frequency noise reduction provided by the chevron nozzle becomes almost negligible, whereas the increase of high-frequency noise becomes substantial and the shielding effect is observed to decrease.

1. Introduction

Jet noise has been significantly reduced over the years, mainly due to an increase in the bypass-ratio (BPR) in turbofan engines, which reduces the velocity gradient and, consequently, the shear stresses within the shear layer of exhausted jets. An increase in the nacelle diameter, as found in modern high-BPR engines, has allowed aircraft to operate with decreased exhaust flow velocities without impacting the thrust [1]. These engines are capable of operating with BPR values of up to 17 under cruise conditions [1], with acoustic emissions improved by 20 EPNdB and 50% less specific fuel consumption when compared to the first-generation turbojet engines [2]. Nevertheless, the exhaust jet remains a major source of aircraft noise, particularly during takeoff. Further noise reduction by increasing the BPR does not seem to be viable due to a number of drawbacks, such as difficulties associated with the nacelle integration, weight increase and nacelle drag, which may compromise the fuel consumption benefits [1,2].

The search for even quieter aircraft has led the aviation industry to test innovative strategies including non-conventional aircraft designs [3], distributed propulsive systems [4] and the use of porous material under the wing [5]. Although these strategies seem promising for reducing noise, they have several practical limitations, particularly during the manufacturing process, besides retrofit issues. Therefore, alternative strategies for noise reduction that do not considerably affect the manufacturing process must be further explored.

Over the years, many experimental studies have been performed in order to assess potential technologies for the reduction of jet noise [6–9]. Among these technologies, the use of chevrons at the trailing edge of turbofan engines has been successfully applied to increase the mixing of jet flows [10] and for jet noise reduction [11,12]. These devices induce streamwise vorticity in the shear layer, leading to enhanced mixing and reduced potential core length [13–15]. Additionally, chevrons reduce low-frequency noise [14,15], which is commonly associated with large-scale structures in the flow, and increase high-frequency noise, usually

* Corresponding author.
E-mail addresses: lpb@polo.ufsc.br (L.P. Bastos), deschamps@polo.ufsc.br (C.J. Deschamps), andrey.rs@ufsc.br (A.R. da Silva).

http://dx.doi.org/10.1016/j.apacoust.2017.06.008
0003-682X/

Nomenclature

c_{amb}	speed of sound under ambient conditions
c_j	speed of sound under the conditions inside jet plume
Dj	exit nozzle diameter/jet diameter
f	frequency
h	radial position/vertical height
BPR	bypass-ratio
M_a	acoustic Mach number
M_j	local Mach number
NPR	nozzle pressure ratio
P_t	total pressure
P_{amb}	ambient pressure
PSD	power spectral density
PR	power ratio
SPL	sound pressure level
T_j	jet temperature
T_{amb}	ambient temperature
TR	temperature ratio
U_j	jet velocity
X_s	surface length

attributed to small-scale turbulent structures [14]. This is accompanied by the shifting of the flow noise sources to regions closer to the nozzle and the peak noise to higher frequencies [16]. Hence, noise reduction using chevron nozzles is essentially achieved by shifting the acoustic energy to higher frequencies, which are more easily attenuated by the atmosphere when compared to the low frequency content.

It has been shown that significant noise reductions of up to 2.7 dB EPNL can be achieved using core and fan nozzles with chevrons in comparison to a baseline (round) nozzle, at the expense of minimal thrust loss [17]. The chevron technology has been constantly evolving in the search for greater aerodynamic efficiency and noise reduction [18–20]. Currently, the latest generation of chevrons is designed to also take into account the shock cell noise [21] and the installation effect caused by the position of the engine on the aircraft [19,20].

Although studies to investigate the effect of chevrons on the flow and acoustic field have been elucidative, they have generally been carried out by considering isolated jet tests [15,17,18]. In the installed configuration, important interactions take place between the exhaust jet and airframe components, such as the wing, pylon and high-lift devices. These interactions generate additional noise sources and modify the resultant noise signature [22,23]. For instance, the interaction between the pylon and the exhausted jet creates flow features that are not present in the isolated case [23]. These features interfere with the performance of noise suppressing devices such as chevrons [23,24]. Another instance takes place if a jet is in close proximity to the wing so that the entrainment properties of flow are changed [25], leading to flow deflection and enhanced levels of turbulence [26,27]. Consequently, this results in intensified acoustic scattering and augmented noise levels [28]. Moreover, the shielding effect, which is dependent on the mounting side of the engine with respect to the wing (above or below), plays an important role in determining the amount of sound radiated to the surrounding community [29–31]. The results of the experimental study suggest that the far-field noise produced by an installed jet issued from a baseline nozzle is significantly increased by reducing the nozzle-to-wing gulley height, as well as by increasing the flap angle with respect to the jet [32]. Additional investigations have shown that the presence of an angled flap near the jet increases the noise levels by up to 9 dB at sideline measuring points [33].

In fact, previous studies on chevrons [10,11,13–17] and installation effects [18,22,29–33] have provided an interesting framework to understand the mechanisms involved in noise generation by jet engines. Nevertheless, little is known about the combined effect of jets with chevron nozzles in close proximity to the wing [19,32,34].

The goal of this study was to investigate the combined effect of installed jets with chevron nozzles. The experimental investigation was based on a fundamental setup involving a jet-over-wing mounting configuration, from which the influence of chevrons on the jet-surface noise and on the shielding effects was assessed. For these configurations, adequate engine positioning in relation to the airframe is crucial in achieving reduced noise levels [35–37]. The analysis herein is accomplished through measurements of the far-field noise produced by cold subsonic jets issued from baseline and chevron nozzles installed under a flat plate at different cord (surface length) and vertical positions (radial positions). The experiments were conducted for Strouhal values varying from 0.1 to 10, corresponding to a frequency range between 0.4 and 40 kHz and Mach numbers ranging from 0.5 to 0.9.

This paper has been organized into various sections. The section 'Material and Methods' provides details on the test setup adopted in this investigation. The following section, 'Results and Discussion' presents the validation of the experimental setup and results for weakly-integrated cases that take into account the nozzle types SMC 000 and SMC 006 [15]. Additionally, the results for these two nozzle geometries are presented for highly-integrated configurations in the following sub-section. Finally, the section 'Conclusions' summarizes the main findings of this study.

2. Material and methods

The experiments were conducted at a jet rig facility of the Federal University of Santa Catarina [38] as depicted in Fig. 1. The facility is composed of a conditioning unit {1} consisting of a compressor, a heatless air dryer and a filter unit, connected to a 15 m^3 air reservoir {2}. This system controls the air humidity, eliminates the presence of solid particles and supplies a flow of steady dry air at controlled temperature and pressure. The air flow from the reservoir is controlled by an automated system composed of block and control valves {3} to avoid pressure fluctuations and allow for emergency shut-off of the air supply, if necessary. Before reaching the test chamber, the air flow passes through a plenum {4} in order to reduce the noise generated in the upstream pipeline due to flow unsteadiness. The thermodynamic properties of air inside the plenum are used to evaluate the acoustic Mach number of the jet based on the isentropic flow condition. The flow line terminates in a 6-inch flange that allows for the connection of different nozzles. In the present work, tests were performed using 2-inch exit diameter nozzles (D_j), originally investigated by Bridges and Brown [15], with and without chevron (SMC 006 and SMC 000, respectively). The tests are carried out in a 60 m^3 fully anechoic chamber {5} with a cut off frequency at around 400 Hz. The far-field sound is acquired from an arc-shaped array containing ten free-field 1/4″ microphones distributed from 60 to 150 degrees at 10 degree intervals. The array of microphones is centered on the nozzle exit at a radial distance of 2.33 m ($\sim$44 D_j) in order to ensure a far-field condition. The measurements were conducted with a multichannel acquisition card having a maximum sampling rate of 204.8 kS/s per channel. Data acquisition was performed by a Lab-

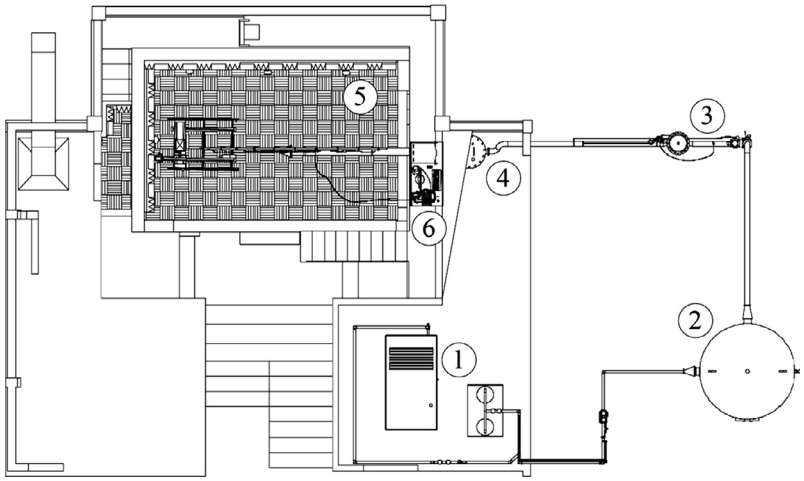

Fig. 1. Jet rig facility at the Federal University of Santa Catarina. 1 – Conditioning unit, 2 – Air reservoir, 3 – Block and control valves, 4 – Plenum, 5 – Test chamber, 6 – Control room.

View routine using intervals of 8 s, a 3 Hz high-pass filter and a sampling rate of 120 kHz. All facility operations are executed from a control room next to the test chamber {6}.

The measurements were carried out with two main objectives: (**i**) to assess the effect of surface length (X_s) and radial position (h) on the jet noise; and (**ii**) to determine how the chevrons modify the resulting noise associated with installed configurations (Fig. 2).

Experimental data available in literature for installed jets issued from nozzle SMC 000 near a flat plate under different flow conditions were adopted to validate our measurements [39]. Table 1 provides information on the flow conditions investigated for the nozzle without chevrons (SMC 000) and for the chevron nozzle (SMC 006). Approximately the same flow conditions were used to measure the jet noise originating from both nozzles located at different positions in relation to the flat plate (Table 2).

The plate was made of aluminum segments (0.5″ thickness) that could be connected to each other in order to change the plate effective length, as depicted in Fig. 2. The total span of the plate was 30 D_j (∼1.524 m) and the maximum length was 21.6 D_j (∼1.097 m). The trailing edge of the plate was milled with a chamfer of approximately 45° to produce a sharp end oriented in the same direction as the flow. The plate was mounted on an automated arm, which controlled its movement in the radial direction, h/D_j, from 0.0 to 6.0, and in the axial direction, X_s/D_j, from 0.65 to 21, both the directions are normalized by the nozzle exit diameter.

The first two segments of the plate are attached to the positioning system and are always in place. The plate can be freely moved backwards along the x axis when $h/D_j \geqslant 2.0$, allowing $0.65 \leqslant X_s/D_j \leqslant 12$, but this is not the case for $h/D_j \leqslant j$ 1.0 due to the presence of the nozzle. Hence, when h/ Dj ⩽ 1.0, the leading edge of the plate is placed in line with the nozzle exit plane and the surface lengths X_s/D_j of 14.5 and 21 are obtained by using the plate with two and three segments, respectively, combined with the shorter segment of the trailing edge.

In the first set of experiments, weakly-coupled installation configurations ($2.0 \leq h/D_j \leq 6.0$) were tested with 8 different surface lengths from $X_s/D_j = 0.65$ to $X_s/D_j = 12$, as shown in Table 2. In the second set of tests highly integrated installation configurations

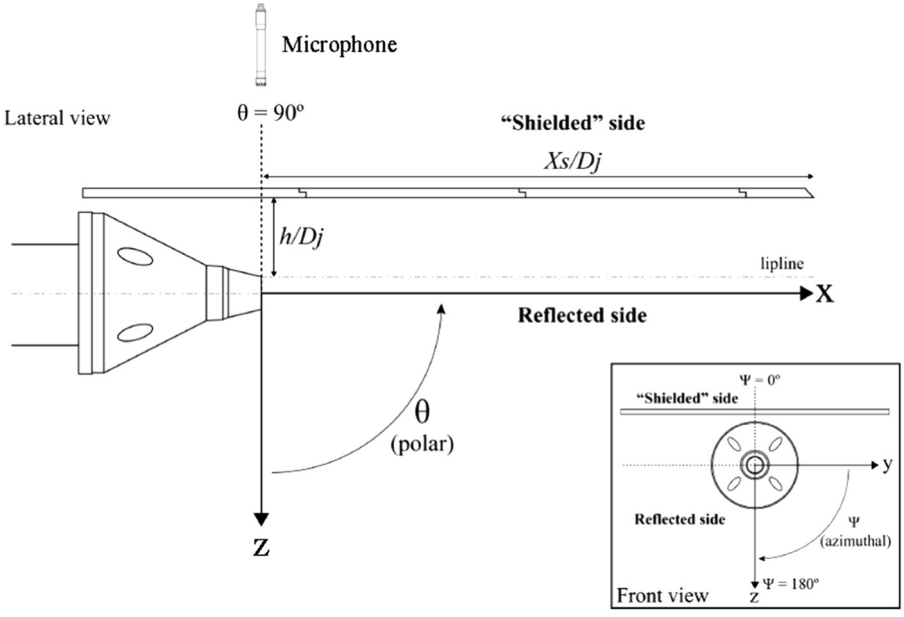

Fig. 2. Coordinate system adopted and nomenclature used to describe surface lengths (X_s/D_j) and radial positions (h/D_j) investigated.

Table 1
Setpoints, nozzle geometries and jet operating conditions.

Cases	Nozzle	NPR (P_t/P_{amb})	TR T_j/T_{amb}	M_a (U_j/C_{amb})	M_j (U_j/C_j)
1	SMC 000	1.200	0.988	0.5	0.516
2	SMC 000	1.301	0.966	0.6	0.625
3	SMC 000	1.452	0.875	0.7	0.749
4	SMC 000	1.633	0.913	0.8	0.867
5	SMC 000	1.855	0.891	0.9	0.983
6	SMC 006	1.202	0.916	0.5	0.519
7	SMC 006	1.304	0.938	0.6	0.627
8	SMC 006	1.439	0.904	0.7	0.739
9	SMC 006	1.619	0.866	0.8	0.858
10	SMC 006	1.858	0.832	0.9	0.984

Table 2
Surface lengths (X_s/D_j) and radial positions (h/D_j) used in measurements of installed jet.

Cases	Surface lengths (X_s/D_j)	Radial positions (h/D_j)
1 to 10	0.65	2.0, 3.0, 4.0, 6.0
1 to 10	1.35	2.0, 3.0, 4.0, 6.0
1 to 10	2.0	2.0, 3.0, 4.0, 6.0
1 to 10	4.0	2.0, 3.0, 4.0, 6.0
1 to 10	6.0	2.0, 3.0, 4.0, 6.0
1 to 10	8.0	2.0, 3.0, 4.0, 6.0
1 to 10	10.0	2.0, 3.0, 4.0, 6.0
1 to 10	12.0	2.0, 3.0, 4.0, 6.0
1 to 10	14.5	0.0, 0.5, 1.0
1 to 10	21	0.0, 0.5, 1.0

($0.0 \leq h/D_j \leq 1.0$) were assessed for two surface lengths, namely $X_s/D_j = 14.5$ and 21. For the far-field acoustic measurements the surface was placed above the nozzle, as shown in Fig. 2. The "shielded" side of the plate was chosen for carrying out the experiments for several reasons. Firstly, the diffraction effect caused by the trailing edge is more significant on this side [40]. On the reflected side, the sound waves due to the interaction of the jet and the trailing edge need to cross the jet flow before they reach the microphones. Thus, information related to the frequency content and noise level can be lost due to blockage and refraction effects [25,41,42]. Secondly, there is great similarity between the power spectral densities of the shielded and reflected sides of the plate as far as low frequency is concerned [25].

Moreover, the position of the plate allows the determination of the installation effects associated with current strategies which involve changes in the aircraft design, such as installing the engine above the wing. In addition, Fig. 2 shows the reference system for the x, y and z coordinates, which are normalized to the nozzle exit diameter (D_j). As can be seen, the system origin is located on the centerline of the nozzle exit plane. The positive direction of the x-axis points to the main jet stream, whereas the y-axis is parallel to the surface and the z-axis is normal to the surface.

The noise data presented next refer to the microphone at a polar angle, θ, of 90° and an azimuthal angle, Ψ, of 0°. Therefore, the sound propagation effects can be neglected. Acoustic measurements were conducted at a distance of 44 Dj (~2.23 m) from the nozzle exit and scaled to 100 D_j without applying a correction for atmospheric attenuation.

A total of 380 jet configurations were tested with different nozzles and Mach numbers ranging from 0.5 to 0.9. In order to compare the results with those provided in previous literature, noise data were acquired in terms of narrow-band Power Spectral Density (PSD) with a resolution of 10 Hz and converted into 1/12 octave bands as a function of the Strouhal number ($St = f\ D_j/U_j$). The 1/12 octave bandwidth was chosen in order to track the peak noise behavior for different configurations.

3. Results and dicussion

This section initially presents a comparison between the current results and those provided by the literature in terms of PSD, considering only the baseline nozzle (SMC 000), for the purpose of validation. Thereafter, the results for weakly and highly integrated jet-plate configurations considering both baseline and chevron nozzles are compared and discussed.

3.1. Validation of experimental data

Results for PSD were obtained for installed jets issued from the nozzle without chevrons (SMC 000) and compared with the data reported by Brown [39]. Fig. 3 shows such measurements for $M_j = 0.516$, $X_s/D_j = 6$. Brown [39] did not report the data for the radial position $h/D_j = 2$, however two similar positions were used in comparison for this paper's study, namely $h/D_j = 1.6$ and 2.5. Despite these differences in the h/D_j value, good agreement was found with deviations smaller than 1 dB for most of the Strouhal number range. The greater difference observed between the PSD curves at low Strouhal numbers is associated with the fact that noise levels are more sensitive to the plate radial position h/D_j at low frequencies, whose values are different for the three curves. This phenomenon seems to be associated with a distribution of dipoles at the trailing edge caused by the direct interaction of

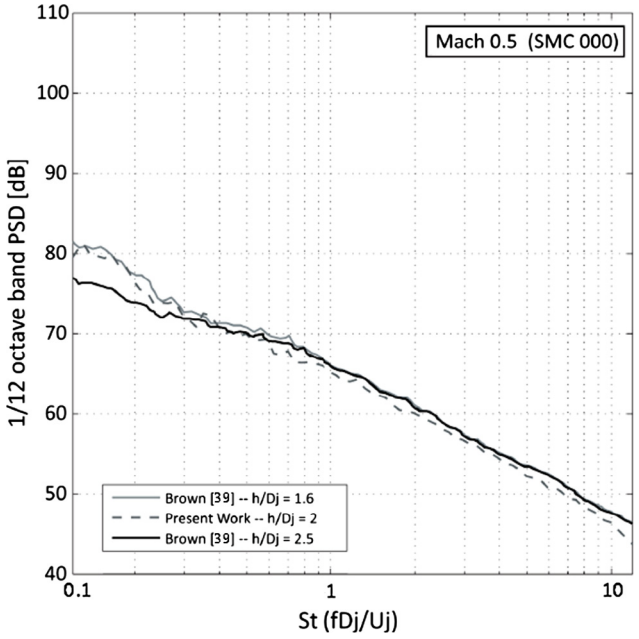

Fig. 3. PSD results obtained in this study ($M_j = 0.516$; $X_s/D_j = 6$ and $h/D_j = 2.0$) and by Brown [39] ($M_j = 0.513$; $X_s/D_j = 6$ and $h/D_j = 1.6$ and 2.5).

the jet plume with the plate, as firstly reported by Head and Fisher [43] and more recently by Lawrence [25].

3.2. Installed jets from nozzles SMC 000 and SMC 006: Weakly-integrated configurations

The measurements revealed that the installation effect due to the presence of the plate is significant only for configurations with $X_s/D_j \geq 2$, when $2 \leq h/D_j \leq 6$. Moreover, the most significant increase in terms of PSD takes place for $h/D_j = 2$. This implies that the plate modifies the resulting PSD curve without interacting directly with the hydrodynamic near-field of the jet. These observations are coherent with results presented by Cavalieri et al. [44] and Brown and Wernet [45]. In contrast, for configurations with $X_s/D_j < 2$ and $2 \leq h/D_j \leq 6$, the results were found to be similar to those observed for isolated jets (data for these configurations are not reported here).

Fig. 4 shows the PSD results for the isolated and installed configurations, with $X_s/D_j = 8$ and $h/D_j = 2$, for the nozzle without chevrons (Fig. 4a) and for the nozzle with the chevron termination (Fig. 4b). When compared to the isolated cases, the increases in PSD found in the low-frequency region seen in Fig. 4a and b are attributed to sound diffraction and acoustic scattering generated by the plate. The combination of these effects is referred to here as jet-surface interaction noise. It should be noted that the noise data presented in Fig. 4 were adjusted to a single plot. Interestingly the increases in PSD due to the jet-surface interaction for Mach 0.5, as seen in Fig. 4a, are restricted to a narrow range of Strouhal numbers. Nevertheless, they present significant differences in magnitude when compared to the respective isolated case.

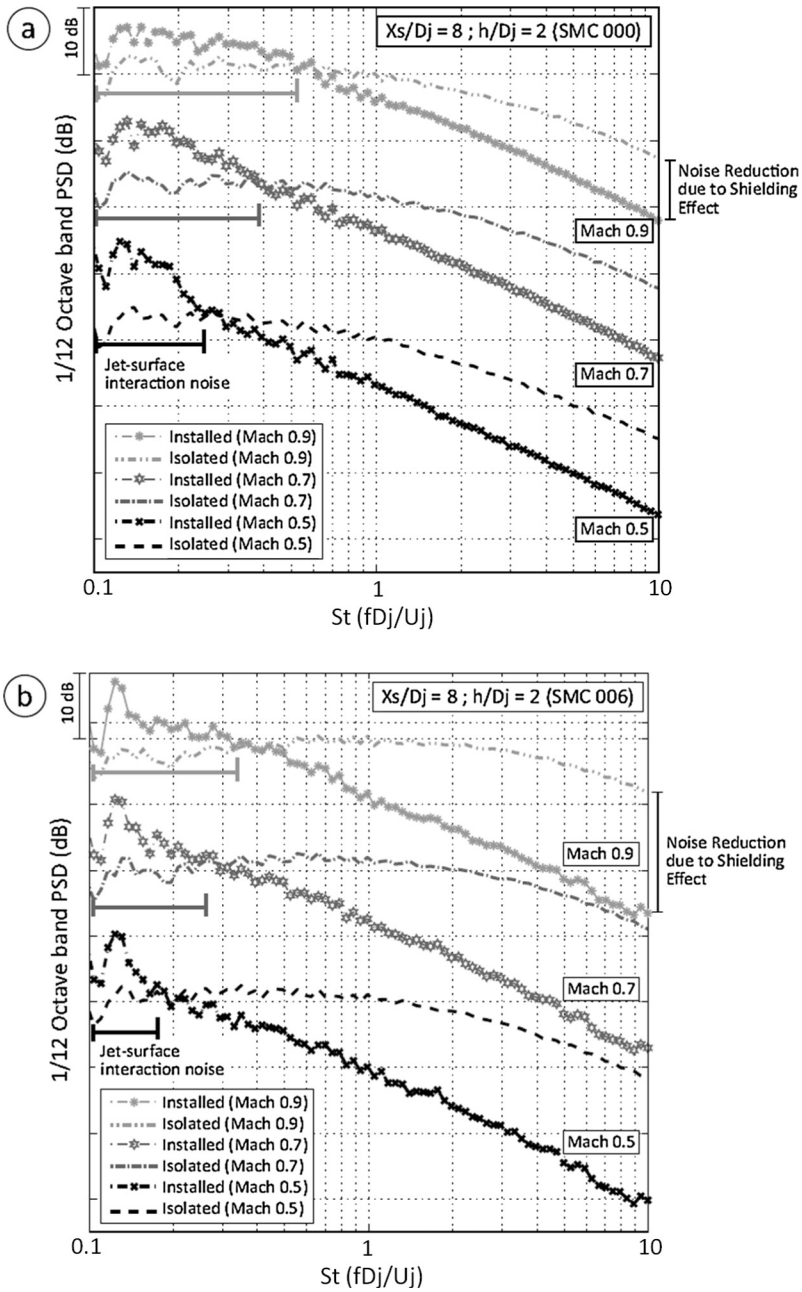

Fig. 4. PSD results for isolated and installed jet configurations with $X_s/D_j = 8$ and $h/D_j = 2$ considering Mach numbers of 0.5, 0.7 and 0.9: (a) nozzle SMC 000 and (b) nozzle SMC 006.

As the Mach increases to 0.9, the differences in the noise levels for installed and isolated cases become smaller and the Strouhal range at which the PSD increase takes place becomes wider. This can be explained by the dependence of prevailing sound sources on the jet velocity in each situation. Under isolated jet conditions the noise levels are solely associated with the turbulent mixing, which are characterized by quadrupole sources with sound intensity proportional to the eighth power of the jet velocity ($\propto U_j^8$). On the other hand, when the surface is close to the jet in the installed configuration, dipole-type sources are dominant when $M \to 0$, since their sound intensity varies with values between the fifth and sixth powers of the jet velocity ($\propto U_j^5$ to U_j^6), depending on the trailing edge geometry [46]. In fact, one can express the power ratio, *PR*, between the acoustic powers produced by dipoles and quadrupoles in terms of Mach number by $PR \sim 1/(Mc)^3$, where c is the constant speed of sound. This expression for *PR* shows that the contribution of dipoles exceeds that of quadrupoles by a factor of $\sim 1/M^3$, i.e., it becomes more significant as $M \to 0$. Therefore, the sound intensity of quadrupole and dipole sources increase with the jet velocity, but their relative difference is reduced as $M \to 1$. Hence, the contribution of dipole sources to the PSD is much greater than that of the quadrupole sources for Mach number of 0.5.and decreases as $M \to 1$. This explains the greatest difference in the PSD values for the installed and isolated jet cases at Mach 0.5. As the Mach number is increased to Mach 0.9, the difference between the contributions from quadrupole and dipole sources decreases and the difference between the noise levels of installed and isolated jet configurations is reduced. This is an expected behavior according to Lawrence et al. [47] and Brown [39,48].

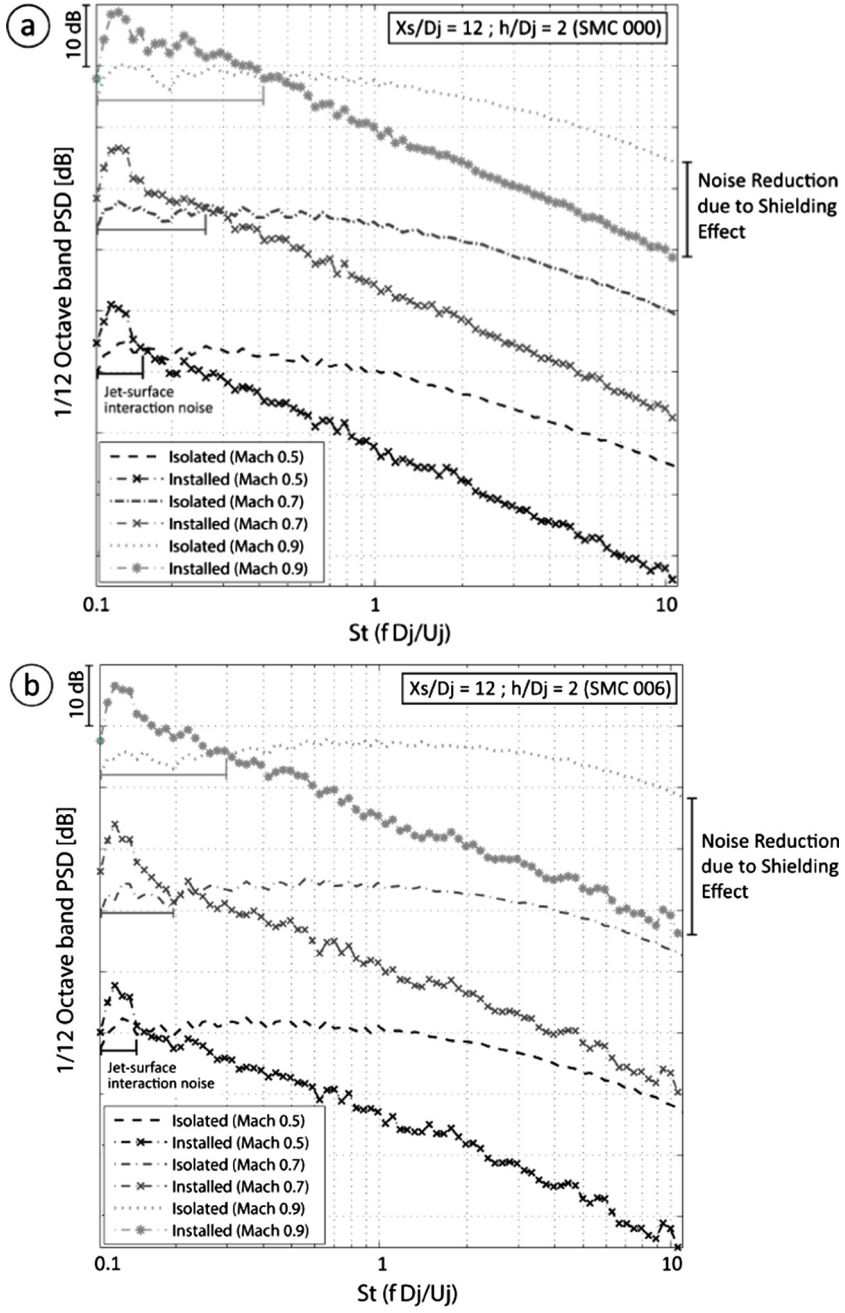

Fig. 5. PSD results for isolated and installed jet configurations with $X_s/D_j = 12$ and $h/D_j = 2$ considering Mach numbers of 0.5, 0.7 and 0.9: (a) nozzle SMC 000 and (b) nozzle SMC 006.

Fig. 4b shows a similar behavior for the PSD values associated with the chevron nozzle (SMC 006) and the same installation configuration ($X_s/D_j = 8$ and $h/D_j = 2$). However, the increase in the noise associated with the chevron nozzle takes place at a narrower Strouhal region when compared with the baseline nozzle. Moreover, the difference between the noise levels of installed and isolated cases slightly increases in proportion to the Mach number. This is the opposite of that observed for the baseline nozzle. This phenomenon is related to the jet spreading caused by the chevrons, which acts to thicken the vortex sheet as the Mach number is increased. It has been thoroughly discussed that, for isolated jet cases, the effectiveness of chevrons in noise reduction increases with the Mach number [49]. Nevertheless, for the installed jet condition, particularly when $X_s/D_j = 8$ and $h/D_j = 2$, the increase in Mach number implies an increase of acoustic scattering and reduces the sound diffraction, thereby limiting the noise increase to low Strouhal values. Additionally, as can be seen in Fig. 4b, the maximum difference between the PSD curves of installed and isolated configurations does not change significantly with the Mach number in the range $0.1 \leq St \leq 0.2$, remaining at around 10 dB.

At high Strouhal numbers, the noise reduction for the chevron nozzle is significantly higher than that of the baseline nozzle. This result is consistent with the observations of Nikam and Sharma [16] and can be explained, as previously mentioned, by the concentration of high frequency sound sources (small turbulence scales) at a region closer to the nozzle exit. This acts to enhance the role of the plate as an efficient sound barrier, given that high-frequency sources have a low diffraction capability. Therefore, in comparison to the nozzle without chevrons (SMC 000), a greater noise reduction due to shielding effect can be achieved with the chevron nozzle (SMC 006) for the same surface length. Likewise, the same noise reduction can be achieved for nozzles with and

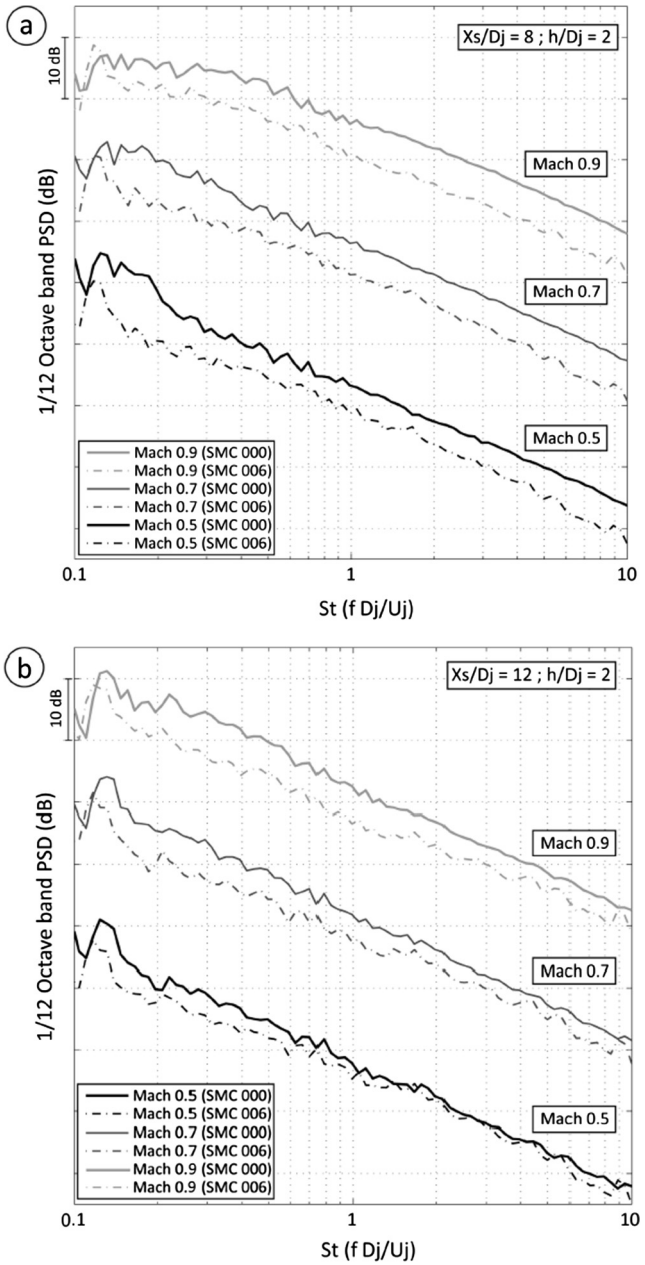

Fig. 6. Comparison of PSD results for nozzles SMC 000 and SMC 006: (a) $h/D_j = 2$; $X_s/D_j = 8$; (b) $h/D_j = 2$; $X_s/D_j = 12$.

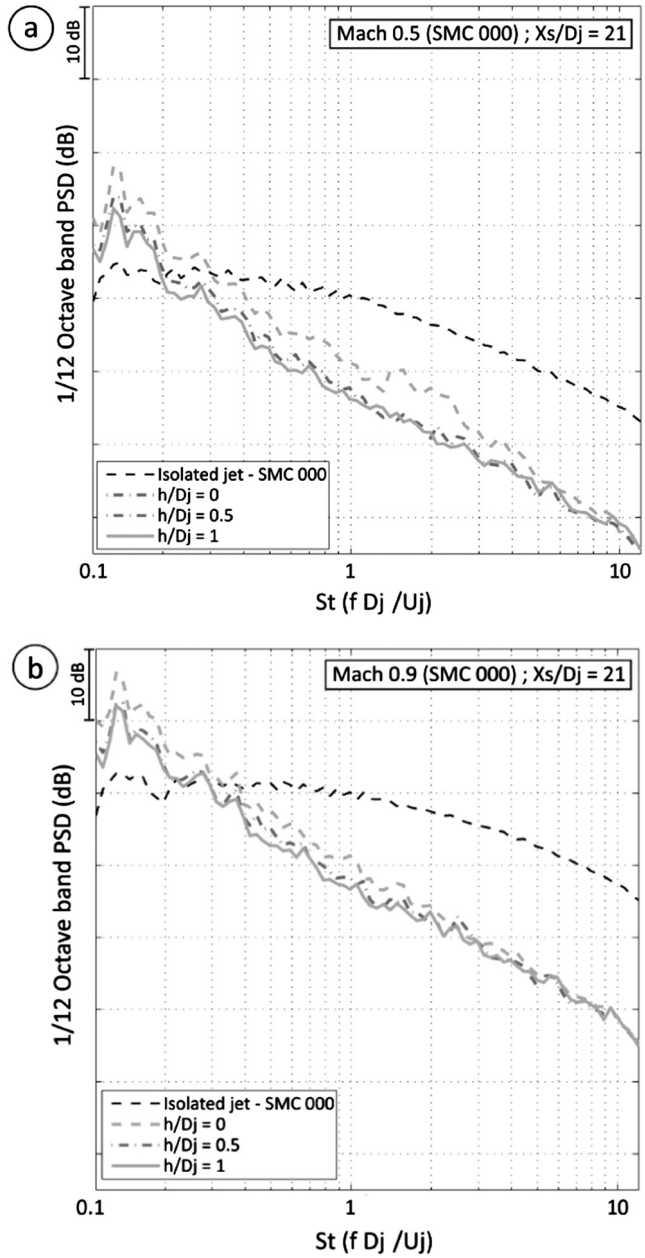

Fig. 7. PSD results for highly integrated configurations with $X_s/D_j = 21$ and $h/D_j = [0.0,0.5,1.0]$ considering nozzle SMC 000: (a) Mach 0.5 and (b) Mach 0.9.

without chevrons when considering a shorter surface length for the first case.

For long surface lengths ($X_s/D_j = 12$) and the same radial position ($h/D_j = 2$) shown in Fig. 5, the jet plume begins to interact directly with the surface trailing edge for both nozzles tested. In this situation, the sound diffraction is reduced due to the increase in surface length. On the other hand, this direct interaction between the jet and the trailing edge significantly increases the acoustic scattering caused by the plate and creates a jet redirection. As a result, the noise reducing performance of the chevron nozzle is diminished but the overall acoustic benefits are kept to some extent. This is because the increase of noise associated with the chevron nozzle is still smaller and takes place in a stricter Strouhal range (Fig. 5b) in comparison to the baseline nozzle (Fig. 5a). This phenomenon becomes more evident when comparing the results for both nozzles (Fig. 6a and b) with weakly-integrated configurations ($X_s/D_j \geq 2$).

As explained before, the chevron nozzle (SMC 006), in comparison to the baseline (SMC 000), reduces the peak noise that occurs at low Strouhal values and brings about noise reduction throughout the Strouhal range. Such differences in the noise levels are related to the interference caused by the chevron nozzle on sound diffraction and acoustic scattering generated by the plate for the different installation configurations analyzed.

3.3. Installed jets from nozzles SMC 000 and SMC 006: Highly-integrated configurations

This section reports the results for surface lengths with $X_s/D_j = [14.5, 21]$ and radial positions $h/D_j = [0.0, 0.5, 1.0]$, for both the nozzles at Mach 0.5 and 0.9, and with the microphone positioned at polar angle of 90°. The measurements for all of highly-integrated configurations revealed increased noise levels at low Strouhal val-

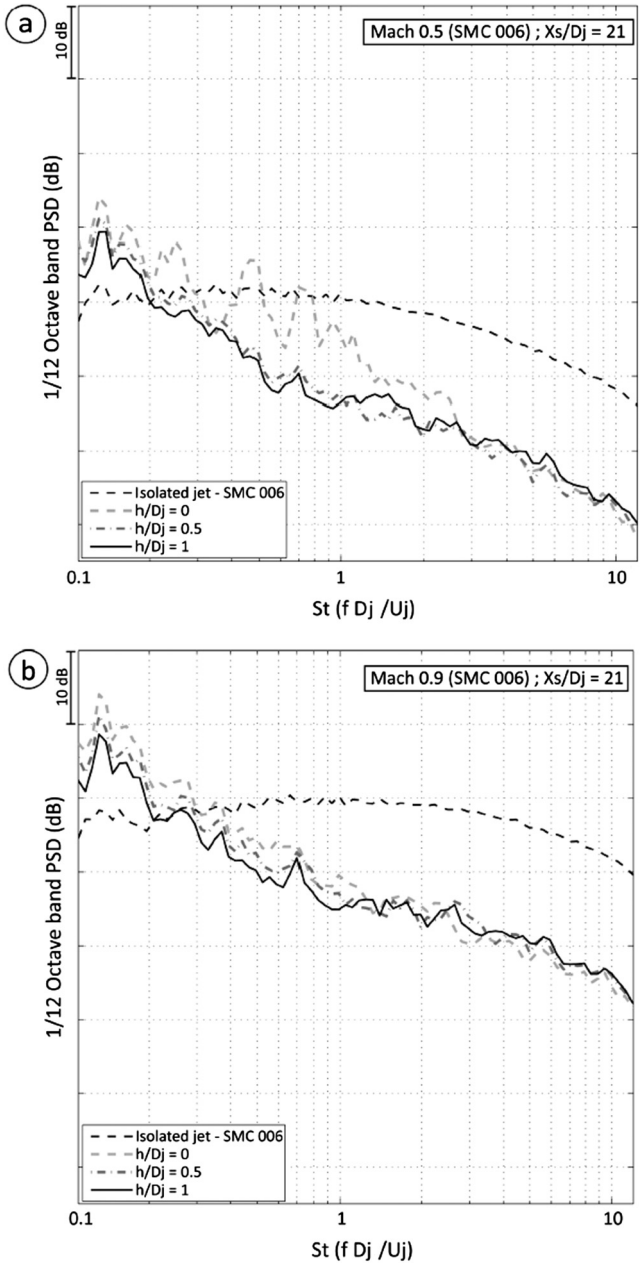

Fig. 8. PSD results for highly integrated configurations with $X_s/D_j = 21$ and $h/D_j = [0.0, 0.5, 1.0]$ considering nozzle SMC 006: (a) Mach 0.5 and (b) Mach 0.9.

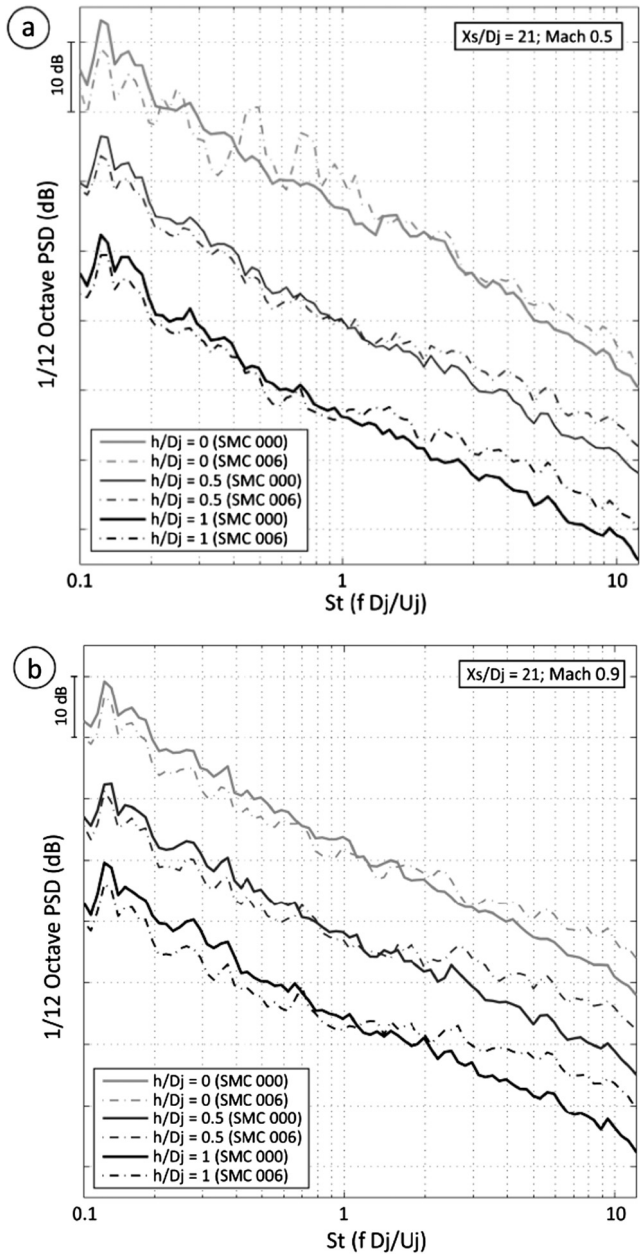

Fig. 9. PSD results for the nozzles SMC 000 and SMC 006 with $h/D_j = [0.0, 0.5, 1.0]$ and $X_s/D_j = 21$: (a) Mach 0.5 and (b) Mach 0.9.

ues, nevertheless, the noise reduction due to the shielding effect at high Strouhal numbers becomes smaller as the radial position decreases. Additionally, slight variations in the radial position led to significant differences in the noise levels. For this reason, the radial distance is considered as the most influential parameter among those analyzed in this work (besides nozzle geometry, surface length and Mach number).

Similar behavior was observed for the two nozzles, particularly in the low-frequency region (St < 0.4). This suggests that, for the Mach number range investigated, the effect of the surface position relative to the nozzle has more influence on the noise levels than the effect associated with the nozzle geometry. According to the PSD values for $X_s/D_j = 21$ and both baseline (Fig. 7a and b) and chevron nozzles (Fig. 8a and b), the increment in noise levels are even more significant and generally take place in an even stricter Strouhal number range (St < 0.3) when compared to the results for weakly-integrated configurations. This might be explained by the length of the surface, through which only long wavelengths (i.e. low frequencies) can be diffracted. Additionally, when the plate is very close to the flow the surface trailing edge is immersed in the jet plume, thus enhancing the acoustic scattering and intensifying the jet redirection. This acts to increase the noise levels at low Strouhal values and to restrict the noise reduction due to shielding effect in high Strouhal values. The PSD results for the surface length equal to $X_s/D_j = 14.5$ are very similar to those for $X_s/D_j = 21$ and, for this reason, these data are not presented in this paper. However, it is important to mention that the behavior of the chevron nozzle at Mach 0.5 and $X_s/D_j = 21$ is significantly different from the previous cases.

As can be seen in Fig. 8a for values of $h/D_j = 0.5$ to $h/D_j = 0.0$ and Mach 0.5, considerable increases in the noise levels are observed at mid Strouhal values. However, this increase of noise level at mid Strouhal number is not visible when the Mach number is increased to 0.9 (Fig. 8b). The same phenomenon has been recently observed by Lawrence [25]. As firstly reported by Head and Fisher [43], the broadband increase in the low-frequency region, as indicated in Fig. 8a, particularly for h/D = 0, seems to be associated with a distribution of dipoles at the trailing edge caused by the direct interaction of the jet plume with the plate. This effect increases as h and M decrease. On the other hand, when $M \rightarrow 1$, the contributions of quadrupole sources become significant. As a consequence, the contribution of quadrupoles on the PSD acts to mask the dipole effect. For this reason, the low-frequency increase caused by the dipole distribution cannot be clearly identified in Fig. 8b. In other words, there appears to be a limit to the proximity between the chevron nozzle and the surface which must be respected in order to preserve the acoustic benefits obtained from the use of chevrons, particularly in the medium Strouhal values and lower Mach numbers.

For the same configuration ($X_s/D_j = 21$ and $h/D_j = [0.0, 0.5, 1.0]$) with the chevron nozzle and Mach number of 0.9 (Fig. 8b), the results appear to be similar to those of the baseline nozzle (Fig. 7b) at low Strouhal values. Nevertheless, at high Strouhal values the noise reduction due to the shielding effect is less significant than that for the baseline nozzle. This reduction becomes even smaller as radial position decreases. This trend becomes evident when comparing the results obtained for both nozzles at Mach 0.5 and 0.9 (Fig. 9a and b, respectively).

4. Conclusions

This paper reported an experimental study on jet noise which investigated the combined effects involving a serrated nozzle closely installed to a flat plate for cold subsonic jets. The influence of chevrons on the jet-surface noise and on the shielding effect was analyzed for jet-over-wing mounting configurations. For weakly integrated configurations ($2 \leq h/D_j \leq 6$), it was observed that noise levels increase with the surface length and decrease with the radial position, as has also been found in other similar works. Additionally, the differences between the noise levels for isolated and installed jet configurations at low Strouhal values were observed to decrease for the baseline nozzle (SMC 000) and to increase for the chevron nozzle (SMC 006) as functions of the Mach number. For weakly integrated configurations, the chevron nozzle was found to reduce noise levels throughout the Strouhal number and to have more expressive noise reduction due to the shielding effect, particularly for the longer surfaces and higher Mach numbers. On the other hand, for highly integrated jet configurations ($0 \leq h/D_j \leq 1$) the acoustic benefits of chevrons were significantly reduced. In fact, the chevron nozzle was observed to increase the noise levels, mainly at medium and high Strouhal values, as well as to have a reduced shielding effect. This phenomenon is attributed to a higher jet spreading produced by the chevron nozzle which increases the interaction between the flow and the plate and intensifies jet redirection effects. Finally, similar effects on noise levels were observed for all the configurations and nozzles tested, especially in low Strouhal values, for the case of very long surfaces ($X_s/D_j \geq 14.5$) and small values for the radial position ($h/D_j \leq 1$). In such cases, the effect of the surface position relative to the nozzle is stronger than that of the nozzle geometry. The radial position was found to be the most influential parameter which implies that small variations of its value correspond to significant variations in the generated noise, particularly for highly integrated configurations.

Acknowledgment

This study forms part of a joint technical-scientific program of the Federal University of Santa Catarina and EMBRAER established in the Silent Aircraft project. Support from FINEP (Federal Agency of Research and Projects Financing), CNPq (Brazilian Research Council) and CAPES (Coordination for the Improvement of High Level Personnel) is also acknowledged. The authors are also thankful to all members of the technical team involved in the Silent Aircraft project and to James Bridges (NASA Glenn Research Center) for providing the geometry data of nozzles SMC000 and SMC006.

References

[1] Hoheisel H, Von Geyr HF. The influence of engine thrust behavior on the aerodynamics of engine airframe integration. CEAS Aeronaut J 2012;3:79–92. http://dx.doi.org/10.1007/s13272-012-0044-x.
[2] Campos LMBC. On some recent advances in aeroacoustics. Int J Acoust Vib 2006;11:27–45. http://dx.doi.org/10.20855/ijav.2006.11.1190.
[3] Czech MJ, Thomas RH, Elkoby R. Propulsion airframe aeroacoustic integration effects for a hybrid wing body aircraft configuration. Int J Aeroacoust 2012;11:325–68. http://dx.doi.org/10.2514/6.2010-3912.
[4] Gohardani AS. A synergistic glance at the prospects of distributed propulsion technology and the electric aircraft concept for future unmanned air vehicles and commercial/military aviation. Prog Aerosp Sci 2013;57:25–70. http://dx.doi.org/10.1016/j.paerosci.2012.08.001.
[5] Herr M, Rossignol KS, Delfs J, Möβner M, Lippitz N. Specification of porous materials for low-noise trailing-edge applications. In: Proceedings of 20th AIAA/CEAS Aeroacoustics Conference, 2014. http://dx.doi.org/10.2514/6.2014-3041.
[6] Dahl MD, McDaniel OH. The performance of jet noise suppression devices for industrial applications. J Vib, Acoust, Stress, and Reliab Des 1985;107 (3):303–9. http://dx.doi.org/10.1115/1.3269261.
[7] Castelain T, Béra J, Sunyach M. Noise reduction of a Mach 0.7–0.9 jet by impinging microjets. CR Mec 2006;334:98–104. http://dx.doi.org/10.1016/j.crme.2006.01.001.
[8] Alkislar MB, Krothapalli A, Butler GW. The effect of streamwise vortices on the aeroacoustics of a Mach 0.9 jet. J Fluid Mech 2007;578:139–69. http://dx.doi.org/10.1017/S0022112007005022.
[9] Kuznetsov VM. The way to decrease efficiently the noises generated by the jets of passenger aircrafts. Acoust Phys 2010;56:85–95. http://dx.doi.org/10.1134/S1063771010010136.

[10] Bridges J, Wernet, MP. Turbulence measurements of separate flow nozzles with mixing enhancement features. NASA/TM - 211592, 2002. http://dx.doi.org/10.2514/6.2014-3041.
[11] Martens S. Jet noise reduction technology development at GE aircraft engines. In: Proceedings of 22nd congress of international council of the aeronautical sciences, Harrogate, UK, 2002.
[12] Huff DL. Noise reduction technologies for turbofan engines. NASA/TM-214495, Ohio, United States, 2007.
[13] Callender B, Gutmark EJ, Martens S. Flow field characterization of coaxial conical and serrated (chevron) nozzles. Exp Fluids 2010;48:637–49. http://dx.doi.org/10.1007/s00348-009-0751-1.
[14] Gudmundsson K, Colonius T. Spatial stability analysis of chevron jet profiles. In: Proceedings of 13th AIAA/CEAS aeroacoustic conference, 2007. http://dx.doi.org/10.2514/6.2007-3599.
[15] Bridges J, Brown CA. Parametric testing of chevrons on single flow hot jets. In: Proceedings of 10th AIAA/CEAS aeroacoustic conference, 2004. http://dx.doi.org/10.2514/6.2004-2824.
[16] Nikam SR, Sharma SD. Aero-acoustic characteristics of compressible jets from chevron nozzle. In: Proceedings of 20th AIAA/CEAS aeroacoustic conference, 2014. http://dx.doi.org/10.2514/6.2014-2623.
[17] Saiyed NH, Mikkelsen KL, Bridges JE. Acoustics and thrust of separate-flow exhaust nozzles with mixing devices for high-bypass-ratio engines. NASA TM-209948, Ohio, United States, 2000. http://dx.doi.org/10.2514/6.2000-1961.
[18] Mengle VG, Elkoby R, Brusniak L, Thomas RH. Reducing propulsion airframe aeroacoustic interactions with uniquely tailored chevrons: 1. Isolated nozzles. In: Proceedings of 12th AIAA/CEAS aeroacoustic conference, 2006. http://dx.doi.org/10.2514/6.2006-2467.
[19] Mengle VG, Elkoby R, Brusniak L, Thomas RH. Reducing propulsion airframe aeroacoustic interactions with uniquely tailored chevrons: 2. Installed nozzles. In: Proceedings of 12th AIAA/CEAS aeroacoustic conference, 2006. http://dx.doi.org/10.2514/6.2006-2434.
[20] Herkes WH, Olsen RF, Uellenberg S. The quiet technology demonstrator program: flight validation of airplane noise-reduction concepts. In: Proceedings of 12th AIAA/CEAS aeroacoustic conference, 2006. http://dx.doi.org/10.2514/6.2006-2720.
[21] Mengle VG, Ganz UW, Nesbitt E, Bultemeier EJ, Thomas RH. Flight test results for uniquely tailored propulsion-airframe aeroacoustic chevrons: shockcell noise. In: Proceedings of 12th AIAA/CEAS aeroacoustic conference, 2006. http://dx.doi.org/10.2514/6.2006-2439.
[22] Elkoby R. Full-scale propulsion airframe aeroacoustics investigation. In: Proceedings of 11th AIAA/CEAS aeroacoustic conference, 2005. http://dx.doi.org/10.2514/6.2005-2807.
[23] Hunter CA, Thomas RH, Abdol-hamid KS, Pao SP, Elmilingui AA, Massey SJ. Computational analysis of the flow and acoustic effects of Jet-Pylon interaction. In: Proceedings of 11th AIAA/CEAS Aeroacoustic Conference, 2005. http://dx.doi.org/10.2514/6.2005-3083.
[24] Thomas RH, Kinzie KW, Pao SP. Computational analysis of a Pylon-Chevron core Nozzle interaction. In: Proceedings of 7th AIAA/CEAS Aeroacoustic Conference, 2001. http://dx.doi.org/10.2514/6.2001-2185.
[25] Lawrence J. Aeroacoust interact install subsonic round jets Ph.D. Thesis. England: Southampton University; 2014.
[26] Lubert CP. On some recent applications of the Coanda effect to acoustics. Proceedings of Meeting on Acoustics, vol. 11. http://dx.doi.org/10.1121/1.3694201.
[27] Lubert CP. Some recent experimental results concerning turbulent Coanda wall jets. Proceedings of Meeting on Acoustics, vol. 22. http://dx.doi.org/10.1121/2.0000040.
[28] Ffowcs Williams JE, Hall LH. Aerodynamic sound generation by turbulent jet flow in the vicinity of a scattering half plane. J Fluid Mech 1970;40:657–70. http://dx.doi.org/10.1017/S0022112070000368.
[29] Wang ME. Wing Effect on Jet Noise Propagation. In: Proceedings of 6th AIAA Aeroacoustic Conference, 1980. http://dx.doi.org/10.2514/3.57493.
[30] Way DJ, Turner BA. Model tests demonstrating under-wing installation effects on engine exhaust noise. In: Proceedings of 6th AIAA Aeroacoustic Conference, 1980. http://dx.doi.org/10.2514/6.1980-1048.
[31] Berton JJ. Noise reduction potential of large, over-the-wing mounted, advanced turbofan engines. NASA/TM-210025, Ohio, United States, 2000. http://dx.doi.org/10.13140/RG.2.1.1373.9608.
[32] Mengle VG. The effect of nozzle-to-wing gulley height on jet flow attachment to the wing and jet-flap interaction noise. In: Proceedings of 17th AIAA/CEAS Aeroacoustic Conference, 2011. http://dx.doi.org/10.2514/6.2011-2705.
[33] Mead CJ, Strange PJR. under-wing installation effects on jet noise at sideline. In: Proceedings of 4th AIAA/CEAS Aeroacoustic Conference, 1998. http://dx.doi.org/10.2514/6.1998-2207.
[34] Kopiev VF, Faranosov GA, Zaytsev MY, Vlasov EV, Karavosov RK, Belyaev IV, et al. Intensification and suppression of jet noise sources in the vicinity of lifting surfaces. In: Proceedings of 19th AIAA/CEAS Aeroacoustic Conference, 2013. http://dx.doi.org/10.2514/6.2013-2284.
[35] Thomas RH, Burley CL, Olson ED. Hybrid wing body aircraft system noise assessment with propulsion airframe aeroacoustic experiments. Int J Aeroacoust 2012;11:369–410. http://dx.doi.org/10.1260/1475-472X.11.3-4.369.
[36] Doty MJ, Brooks TF, Burley CL, Bahr CJ, Pope DS. Jet noise shielding provided by a hybrid wing body aircraft. In: Proceedings of 20th AIAA/CEAS Aeroacoustic Conference, 2014. http://dx.doi.org/10.2514/6.2014-2625.
[37] Thomas RH, Czech MJ, Doty MJ. High bypass ratio jet noise reduction and installation effects including shielding effectiveness. In: Proceedings of 19th AIAA/CEAS Aeroacoustic Conference, 2013. http://dx.doi.org/10.2514/6.2013-541.
[38] Bastos LP. Development and application of a jet test rig facility for the analysis of installation effects concerning flow and acoustic fields of subsonic jets Ph.D. Dissertation, in Portuguese. Federal University of Santa Catarina; 2016.
[39] Brown C. Developing an empirical model for jet-surface interaction noise. In: Proceedings of 20th AIAA/CEAS Aeroacoustic Conference, 2014. http://dx.doi.org/10.2514/6.2014-0878.
[40] Da Silva FD, Deschamps CJ, Da Silva AR, Simões LGC. Assessment of jet-plate interaction noise using the Lattice Boltzmann method. In: Proceedings of 21th AIAA/CEAS Aeroacoustic Conference 2015. http://dx.doi.org/10.2514/6.2015-2207.
[41] Moore A, Mead C. Reflection of noise from aero-engines installed under an aircraft wing. In: Proceedings of 9th AIAA/CEAS Aeroacoustic Conference. http://dx.doi.org/10.2514/6.2003-3151.
[42] Moore, A, A 3D Prediction of the Wing Reflection of Aero-Engine Noise. Proceedings 10th AIAA/CEAS Aeroacoustic Conference, 2004. http://dx.doi.org/10.2514/6.2004-2865.
[43] Head RW, Fisher MJ. Jet surface interaction noise: analysis of farfield low frequency augmentations of jet noise due to the presence of a solid shield. In: Proceedings 3rd AIAA/CEAS aeroacoustics conference. AIAA Paper 1976–502, 1976.
[44] Cavalieri AVG, Jordan P, Gervais Y. Scattering of wavepackets by a flat plate in the vicinity of a turbulent jet. In: Proceedings 18th AIAA/CEAS Aeroacoustic Conference. http://dx.doi.org/10.1016/j.jsv.2014.07.029.
[45] Brown C, Wernet M. Jet-surface interaction test: flow measurement results. In: Proceedings 20th AIAA/CEAS Aeroacoustic Conference. http://dx.doi.org/10.2514/6.2014-3198.
[46] Crighton DG, Dowling AP, Ffowcs Williams JE, Heckl M, Leppington FG. Modern methods in analytical acoustics. Berlin: Springer-Verlag; 1992.
[47] Lawrence JLT, Azarpeyvand M, Self RH. Interaction between a flat plate and a circular subsonic jet. In: Proceedings 17th AIAA/CEAS Aeroacoustic Conference. http://dx.doi.org/10.2514/6.2011-2745.
[48] Brown C. Jet-surface interaction test: far-field noise results. In: Proceedings of the ASME Turbo Expo 2012: Power for Land, Sea and Air GT2012, Copenhagen, Denmark. http://dx.doi.org/10.2514/6.2014-3198.
[49] Gutmark EJ, Callender B, Martens S. Aeroacoustics of turbulent jets: flow structure, noise sources, and control. Int J Japan Soc Mech Engineers. Series B: Fluids and Therm Eng 2006;49:1078–85. http://dx.doi.org/10.1299/jsmeb.49.107.